Pharm Res (2014) 31:2266–2275
DOI 10.1007/s11095-014-1321-7

RESEARCH PAPER

Directed Self-assembled Nanoparticles of Probucol Improve Oral Delivery: Fabrication, Performance and Correlation

Zhiwen Zhang • Shijun Jiang • Zeying Liu • Baohua Niu • Wangwen Gu • Yaping Li • Jingbin Cui

Received: 19 September 2013 / Accepted: 28 January 2014 / Published online: 4 March 2014

ABSTRACT

Purpose We are reporting on the development of a unique drug delivery platform by directed self-assembly technique to improve the oral delivery of hydrophobic drugs.

Methods Herein, a series of probucol directed self-assembled nanoparticles (PDN) were developed with two components of probucol and surfactant such as Tween 20, Tween 80, D-alpha-tocopheryl polyethylene glycol 1,000 succinate (TPGS) and HS-15, which was respectively named as T_{20}-PDN, T_{80}-PDN, TP-PDN and HS-PDN. The formation of various PDNs was determined by *in vitro* characterization and the physicochemical properties of these PDNs were determined. Moreover, the performance of PDN in enhancing the oral delivery and possible correlation between the *in vitro* properties and *in vivo* performances were investigated.

Results PDN was homogenous nanometer-sized particles with negative surface charge. The cellular uptake of probucol in Caco-2 cell monolayer was respectively increased 1.15, 1.82, 1.59 and 5.31-fold by these PDN. In particular, the oral bioavailability of these PDN was significantly improved 3.0, 4.1, 5.4 and 10.4 folds compared with the free drug suspension. The enhanced cellular uptake and oral bioavailability were correlated with the characters of involved surfactants and the particle size of PDN.

Conclusions Thereby, the directed self-assembled nanoparticles could provide a new strategy for enhancing the oral delivery of hydrophobic drugs.

Z. Zhang • B. Niu • W. Gu • Y. Li (✉)
Center of Pharmaceutics, Shanghai Institute of Materia Medica
Chinese Academy of Sciences
501 Haike Road, Shanghai 201203, China
e-mail: ypli@simm.ac.cn

S. Jiang • Z. Liu • J. Cui
School of Pharmacy, East China University of Science and Technology
Shanghai 200237, China

KEY WORDS correlation · directed self-assembly · nanoparticles · oral delivery · probucol

INTRODUCTION

With few exceptions, the therapeutic efficacy of drugs significantly depends on their systemic exposure following oral delivery (1–3). The orally administered drugs have to be absorbed from the intestine lumen into the systemic circulation or site of action to achieve the pharmacological effects (1,2,4). However, in terms of drug discovery and developments, approximately 40–70% of commercial drugs or drug candidates exhibit extremely low solubility in water and poor absorption in the intestine, which greatly restricted their therapeutic efficacy (1,5–7). As a result, the essential efforts have to be made to improve the oral bioavailability of these poorly water-soluble drugs or drug candidates to acquire the satisfying therapeutic effects.

Directed self-assembly offers a convenient and powerful bottom-up strategy for fabrication of nanoparticles, which presents promising application in sensors, functional materials and molecular biology (8,9). Directed self-assembly of nanoparticle (DSN) can be spontaneously formed with versatile morphological or functional features from small molecules, DNA, oligomers and polymers (8,10). The formation of DSN may ascribe to the intermolecular forces of hydrophobic interactions, hydrogen bonding, electrostatic interactions and π-π stacking among the involved ingredients (8,9,11). A recent report indicated that the self-assembled nanoparticles could be constructed by employing the interactions of aromatic moiety between two small molecules (12). These directed nanoassemblies could provide promising strategies for the entrapment of poorly water-soluble drugs. Up to now, few approaches of directed self-assembly have been exploited in development of drug delivery system.

Nanoparticles have demonstrated tremendous advantages in enhancing the oral absorption of poorly water-soluble drugs (1–3,5,13–16). We hypothesized that the two components of hydrophobic drugs and surfactants could be directed into nanoparticles due to intermolecular hydrophobic interactions between the active agents and lipophilic part of surfactant. In this work, probucol, an insoluble drug (5–10 ng/mL) normally used for the treatment of cardiovascular disease, was selected as a model drug (15,17,18). We tried to fabricate the probucol loaded nanoparticles with probucol and various surfactants by directed self-assembly technique to improve its oral delivery. The formation of probucol directed self-assembled nanoparticles (PDN) was verified by *in vitro* characterization. The cellular uptake in Caco-2 cell monolayer, *in vivo* pharmacokinetic behaviors of various PDN, and possible inherent relationship between *in vitro* properties and *in vivo* performance were determined to evaluate their validity in enhancing the oral delivery of hydrophobic drugs. To our knowledge, this could be the first attempt for development of drug delivery platform by directed self-assembly technique.

MATERIALS AND METHODS

Materials

Probucol (purity 99.7%) was obtained from Wuyi Cihang Pharmaceutical Co. Ltd (Hebei, China). Tween 20 and Tween 80 were purchased from Sinopharm Chemical Reagent Co. Ltd. (Shanghai, China). D-alpha-tocopheryl polyethylene glycol 1,000 succinate (TPGS) was supplied by Sigma-Aldrich (MO, USA). Solutol® HS-15 and Pluronic F68 were provided by BASF Co. Ltd. (Ludwigshafen, Germany). 1,1′-dioctadecyl-3,3,3′,3′-tetramethylindotricarbocyanine iodide (DiR) was obtained from Fanbo Biochemicals Co. Ltd (Beijing, China). All other reagents and solvents were of analytical or high performance liquid chromatography (HPLC) grade.

Cell Culture

Caco-2 cells were obtained from Shanghai Cell Resource Center of Shanghai Institute for Biological Sciences, Chinese Academy of Sciences. Cells were incubated in Dulbecco's Modified Eagle's Medium (DMEM, High Glucose, Gibco, New York, USA) supplemented with 10% (v/v) fetal bovine serum (FBS, Gibco), 2 mM glutamine, 100 units/mL penicillin and 100 μg/mL streptomycin. Prior to the experiment, cells were seeded into a culture plate (24-well, Corning, USA) at 4×10^4 cells/well, and cultured at 37°C in a humidified atmosphere of 5% CO_2. Cells were cultured for 14–16 days to form the cell monolayer for the uptake experiments. The culture media was replaced every other day for the first week and everyday thereafter (19,20).

Animals

Male Sprague–Dawley rats (200–250 g) were supplied from the Sino-British Sippr/BK Lab Animal Ltd. (Shanghai, China). Prior to the experiments, animals were acclimatized at the animal care facility for at least 5 days. The *in vivo* experiments were approved by the Institutional Animal Care and Use Committee (IACUC) of Shanghai Institute of Materia Medica, Chinese Academy of Sciences.

Preparation and Characterization of Probucol Directed Self-assembled Nanoparticles (PDN)

PDN is composed of probucol and surfactant molecules, which is listed in Table I. PDN was prepared by dissolving probucol and surfactant of each formulation (shown in Table I) in anhydrous ethanol with probucol concentration of 5 mg/mL. Then, the mixed solution was evaporated under reduced pressure (0.07 MPa, Heidolph Laborata 4000, Germany) to form a thin film. Afterwards, the film was dispersed into double distilled water by gentle shaking at 37°C. PDN could be spontaneously organized and the terminal concentration of probucol was 20 mg/mL.

The morphology of various PDN was measured under a transmission electron microscope (TEM, JEOL JEM-1230, Tokyo, Japan). Briefly, PDN was diluted with double distilled water and negatively stained with 1% (v/v) uranyl acetate for observation. Samples were loaded onto a copper grid for 2–3 min, rinsed with distilled water, dried at room temperature and imaged under the microscope. The size distribution of PDN was measured by dynamic light scattering (DLS) using a Nano ZS 90 instrument (Malvern, UK). The z-average diameter of PDN, which referred to the intensity average hydrodynamic diameter, was recorded by the accompanied Zetasizer software (Malvern, UK). To investigate the stability of PDN in the gastrointestinal fluids, PDN was diluted with 0.1 N HCl (pH 1.2) or phosphate buffered solution (PBS, pH 6.8), and then analyzed at ambient temperature. Meanwhile, the zeta potential values of various PDN were determined on the same instrument.

Cellular Uptake in Caco-2 Cell Monolayer

Caco-2 cell monolayer is a common *in vitro* model of intestinal membrane for assessing the intestinal absorption of drugs (19). The cellular uptake of PDN was performed in the Caco-2 cell monolayer at 37°C compared with that of probucol solution. Briefly, the cell monolayer was freshly replaced with 1.0 mL of fresh pre-warmed FBS-free DMEM without phenol red and

Table I The Physicochemical Properties of Various Surfactant Molecules and PDN

Surfactant	Structure	MW_T	MW_{LU}-	R_{LT}	HLB	PDN	R_{SP}	MD (nm)	PDI	ζ(mv)
Tween 20	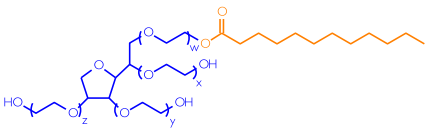	1228	200	0.1629	16.7	T_{20}-PDN	2: 1	44.06	0.124	-10.1
Tween 80	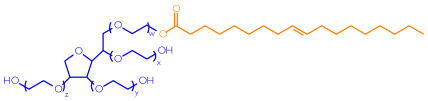	1310	282	0.2153	15.0	T_{80}-PDN	2: 1	53.33	0.283	-9.96
TPGS	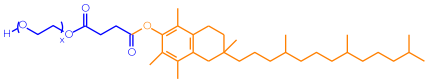	1513	413	0.2730	13.0	TP-PDN	2.5: 1	66.34	0.236	-9.83
HS-15		960	300	0.3125	14-16	HS-PDN	2:1	40.07	0.167	-8.48
Pluronic F68	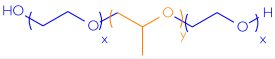	8400	1680	0.2	29	/	3:1	/	/	/

MW_T Molecular weight of total surfactant molecule

MW_{LU} Molecular weight of lipophilic unit of surfactant molecules

R_{LT} Ratio of molecular weight of lipophilic unit compared to that of total surfactant molecule

Rsp Weight ratio of surfactant and pure probucol in various PDN formulations

MD Mean diameter of various PDN

maintained at 37°C for 30 min. Various PDN was added into the culture media with the terminal probucol concentration of 0.25 mg/mL. By contrast, probucol was dissolved in DMSO and added into the culture media to a final concentration of 0.25 mg/mL probucol and 0.5% v/v DMSO. These samples were incubated with the cell monolayer for further 60 min at 37°C. Then, the culture media were removed from each well, centrifuged at 10,000×*g* for 10 min at 4°C (Thermo Biofuge Stratos, Germany) for lactate dehydrogenase (LDH) measurement (GENMED, Shanghai, China) to investigate the biocompatibility of these nanoparticles. Meanwhile, the cell monolayer was carefully collected, homogenized with 0.4 mL of acetonitrile, and centrifuged at 14,000×*g* for 10 min at 4°C (Thermo Biofuge Stratos, Germany). The drug amount in the supernatant was determined by ACQUITY UPLC H-Class system (Waters, USA) on a UPLC® BEH C_{18} column (2.1×100 mm, Ø=1.7 μm, Waters, USA) with the following conditions: mobile phase, acetonitrile-water (94:6, v/v/); flow rate, 0.5 mL/min; column temperature, 40°C; detection wavelength, 242 nm. The relative cellular uptake of PDN was defined as the cellular uptake of various PDN in Caco-2 cell monolayer compared to that of control.

Moreover, the effect of PDN on f-actin filaments of Caco-2 cell monolayer was evaluated under laser confocal scanning microscopy (LCSM, FluoView™ FV1000, Olympus, Japan). Briefly, Caco-2 cells were seeded on the round glass coverslips (Ø10 mm) at 4×10^4 cells/well in 24-well culture plate (Corning, USA), and cultured for 14–16 days as described above. Prior to the experiments, PDN was dispersed in pre-warmed FBS-free DMEM and incubated with the cell monolayer for 60 min at 37°C. At the end point, the cell monolayer was washed twice with cold PBS (pH 6.8) and fixed with 4% buffered paraformaldehyde (w/v) for 10 min at room temperature. The F-actin filaments in each sample were stained with FITC-phalloidin (Sigma) according to the manufacturer's protocol (21). Afterwards, the coverslips were mounted on the glass microscope slides with antifade solution and observed under LCSM (Olympus, Japan). By contrast, the f-actin filaments of cell monolayer without any treatment were performed as a control.

Absorption of PDN in the Intestine

The absorption of PDN in the intestine was measured by *In Vivo* Imaging System (Carestream FX Pro, USA) and LCSM. HS-PDN was used as a typical model, which was fluorescently labeled with a hydrophobic near infrared carbocyanine dye (DiR) in the preparation process as described above (22,23). The fluorescent PDN was orally administered to rats at 200 mg/kg of probucol with 4 mg/kg of DiR. At 1 h and 4 h after oral administration, rats were euthanized and the intestine from duodenum to ileum was carefully removed. Afterwards, the samples were visualized under the *In Vivo* Imaging System with the excitation wavelength of 730 nm and emission wavelength of 790 nm.

Furthermore, to investigate the uptake of PDN in the intestinal villi, PDN was fluorescently labeled with a hydrophobic Nile Red (Acros, New Jersey, USA). The rats were euthanized at 1 h after oral administration of fluorescent PDN. The intestine segments were selected, removed, everted and rinsed with cold PBS (pH 6.8). Then, samples were frozen in embedding media (OCT, SAKURA, Japan) and sectioned at 20 μm (Mev, SLEE, Germany). These sections were rinsed with cold PBS (pH 6.8) and fixed with 2.0% buffered paraformaldehyde for 10 min at room temperature. Then, samples were respectively stained with phalloidin-FITC (Green, Sigma) and DAPI (Blue, Sigma) according to the manufacturer's protocols (19,24). Afterwards, the fluorescence was detected under LCSM and images were captured by FV10-ASW software (Olympus Japan). As control, free fluorescent dye and saline were respectively given to rats and treated as described above.

Pharmacokinetic Behavior of PDN in Rats

The *in vivo* pharmacokinetic behavior of PDN was measured in rats compared with that of free drug suspension. Rats were fasted overnight with free access to water and randomly divided into five groups ($n=4$). Each PDN and free probucol suspension were administered to rats at 200 mg/kg of probucol by oral gavage. Blood samples were collected into heparinized tubes at predetermined time intervals. Plasma was immediately separated by centrifugation at 10,000×*g* for 5 min (Thermo Heraeus, Germany) and stored under −20°C for further analysis.

The plasma samples were treated for further HPLC measurements. Briefly, 350 μL of methanol was added into 50 μL of plasma, vortexed for 60 s and centrifuged at 14,000×*g* for 10 min at 4°C to precipitate the plasma protein. The probucol concentration in the supernatant was determined by HPLC system (Waters 2695–2489, USA) with Eclipse XDB-C_{18} column (150×4.6 mm, I.D. 5 μm, Agilent); the mobile phase: methanol–water (95:5, v/v); flow rate: 1.0 mL/min; detection wavelength, 242 nm. The pharmacokinetic parameters were calculated by non-compartmental analysis. The area under concentration-time curve (AUC) was calculated by the linear trapezoidal rule, while the peak concentration (C_{max}) and the time to C_{max} (T_{max}) were directly obtained from the individual concentration-time data. The relative oral bioavailability (Fr) was defined as the ratio between the $AUC_{(0-t)}$ values of PDN and that of free drug suspension.

Inherent Correlation Analysis

The inherent correlation between the *in vitro* properties of PDN and the relative cellular uptake in Caco-2 cell monolayer or relative oral bioavailability was investigated to clarify the possible mechanism of enhanced oral absorption by the directed self-assembled nanoparticles. The particle size of various PDN and the involved surfactant molecules could be the essential factors affecting the oral absorption of hydrophobic drugs. Four parameters of *in vitro* properties were selected for the correlation analysis, including R_{LT}, R_{LT}/MD, $(R_{LT})^2$, $(R_{LT})^2/MD$. Therein, R_{LT} referred to the ratio between the molecular weight of hydrophobic part of surfactant and that of total surfactant molecules, while MD meant the mean diameter of corresponding PDN (Table I). The linear regression was performed between the relative cellular uptake in Caco-2 cell monolayer or relative oral bioavailability of various PDN and their *in vitro* physicochemical parameters, respectively, and the correlation coefficient was calculated as well.

Statistical Analysis

All statistical analysis was performed using a Student's *t* test. Difference was statistically significant as $p<0.05$, and very significant as $p<0.01$.

RESULTS

Preparation and Characterization of PDN

PDN could be spontaneously organized due to the intermolecular hydrophobic interactions between hydrophobic probucol and lipophilic units of surfactant molecules. The formation of PDN was confirmed by dynamic light scattering (DLS) measurements and transmission electron microscope (TEM) analysis. The experimental results indicated that PDN could be formed by probucol and one of the following surfactants of Tween 20, Tween 80, TPGS or HS-15, which was respectively named as T_{20}-PDN, T_{80}-PDN, TP-PDN and HS-PDN (Table I, Fig. 1). However, the probucol loaded nanoparticles could not be formed with Pluronic F68 (Table I). Accordingly, the formation of drug nanoparticles by directed self-assembly could be closely related with the molecular structure of hydrophobic drugs and lipophilic units of involved surfactant molecules. The physicochemical properties of various PDN were listed in Table I and Fig. 1. The DLS measurements showed that PDN were homogenous nanometer-sized particles with negative surface charge. Meanwhile, the TEM images directly showed nanometric spherical or elliptical particles (Fig. 1), which effectively verified the formation of directed self-assembled nanoparticle by hydrophobic probucol and various surfactant molecules. Moreover, the apparent aqueous solubility of probucol in these PDN was about 20 mg/mL, which was remarkably increased over 2×10^6-fold than that of free probucol. Additionally, the mean diameter of these PDN was not significantly changed when they were respectively diluted with mimicked gastrointestinal (GI) fluids of 0.1 M HCl (pH 1.2) or phosphate

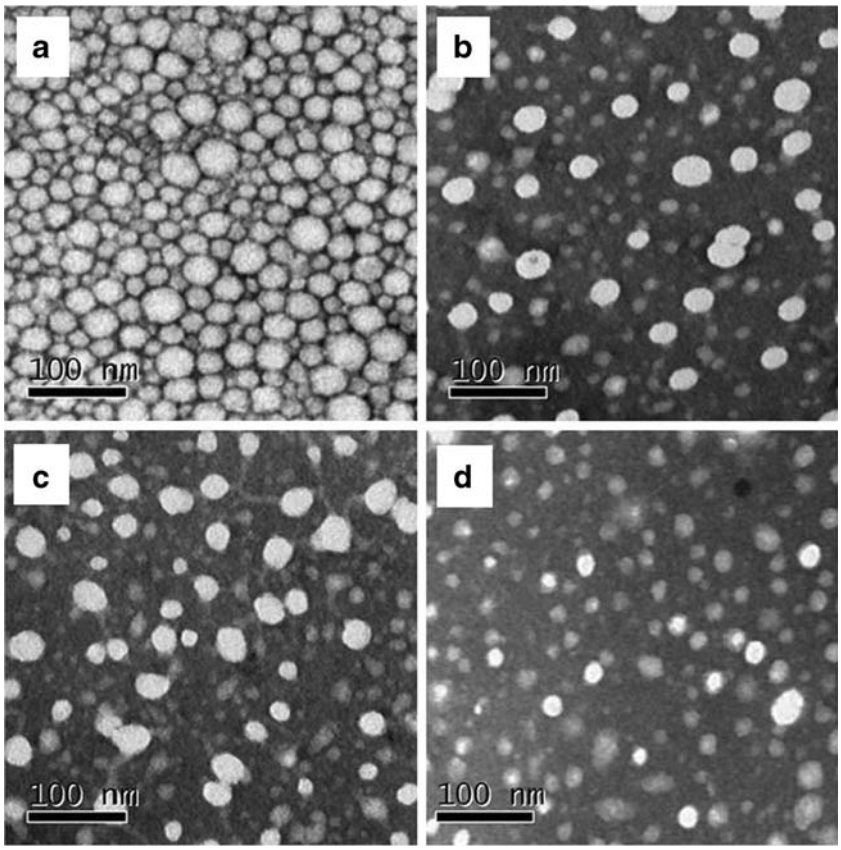

Fig. 1 Typical TEM images of various PDN. (**a**) T_{20}-PDN, (**b**) T_{80}-PDN, (**c**) TP-PDN, and (**d**) HS-PDN.

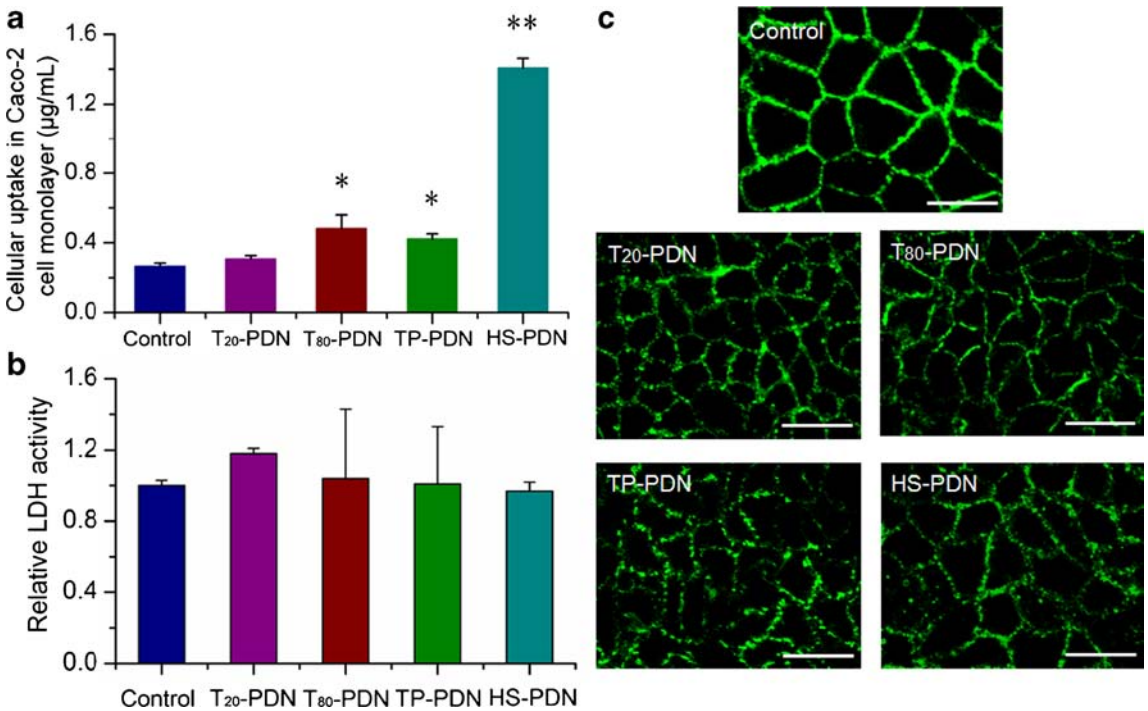

Fig. 2 Cellular uptake of various PDNs in Caco-2 cell monolayers. (**a**) Probucol concentration in Caco-2 cell monolayer treated with various PDN ($^{*}p < 0.05$, $^{**}p < 0.01$); (**b**) Effect of various PDN on F-actin filaments of Caco-2 cell monolayer. The actin filaments was stained with FITC-phalloidin for 60 min at room temperature and observed under LCSM, scale bar = 20 μm.

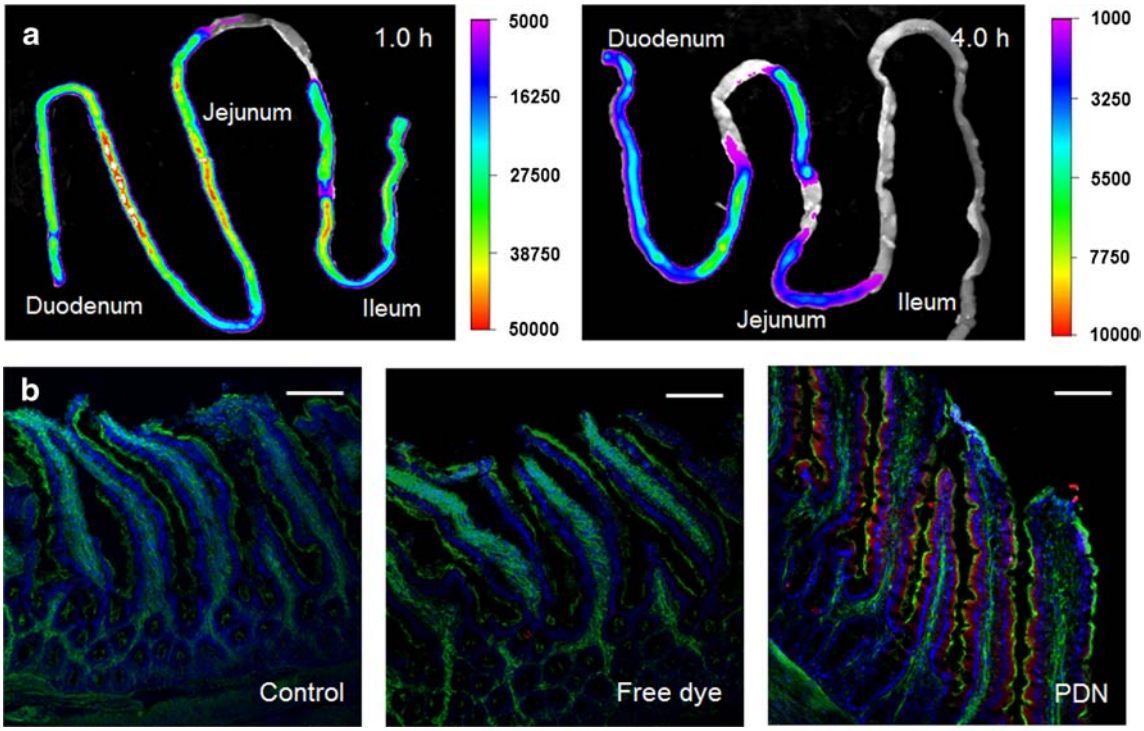

Fig. 3 Absorption of fluorescent PDN in the intestine. (**a**) Distribution of DiR labeled PDN in the intestine at 1.0 h and 4.0 h after oral administration; (**b**) Visualization of Nile red labeled PDN in the intestine epithelium under LCSM, scale bar = 100 μm.

buffered solution (pH 6.8), which indicated the good stability of PDN in GI fluids.

Cellular Uptake of PDN in Caco-2 Cell Monolayer

Caco-2 cell monolayer model is commonly used for measuring the intestinal absorption of active agents and various nano-based drug delivery systems (19,25). The cellular uptake of PDN in the cell monolayer was investigated in comparison with that of probucol solution. At 60 min after incubation, the probucol concentration in the cell monolayer was determined by UPLC analysis (Fig. 2a). The measured results indicated that

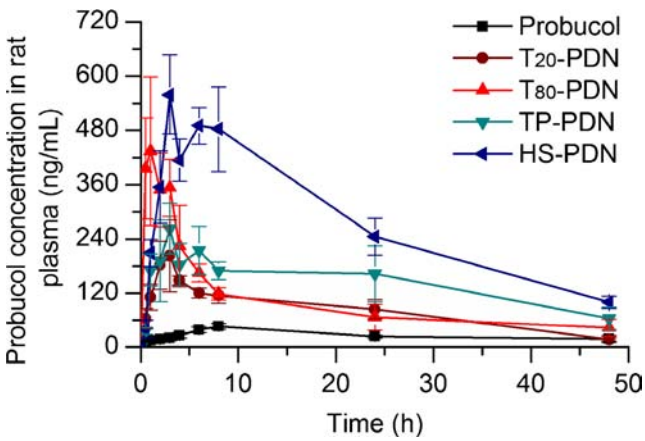

Fig. 4 *In vivo* pharmacokinetic profiles of orally administered PDN and free drug suspension in rats (200 mg/kg).

the cellular uptake of PDN varied with different nanoparticles and significantly depended on the surfactant molecules included in PDN. Briefly, the probucol concentration in Caco-2 cell monolayer was the highest for HS-PDN, then significantly decreased for T_{80}-PDN and TP-PDN, and reduced to the lowest for T_{20}- PDN. The cellular uptake of free drug solution in the cell monolayer was performed as a control. Compared with the free drug solution, the cellular uptake of PDN was increased 1.15, 1.82, 1.59 and 5.31-fold by T_{20}-PDN, T_{80}-PDN, TP-PDN, HS-PDN, respectively. The significant difference among the cellular uptake of these PDNs could result from the characters of different surfactants and the physicochemical properties of their corresponding nanoparticles (3,26).

To evaluate biocompatibility of PDN with the cell monolayer, the activity of LDH in the media was determined by LDH release-assays kit (7). The measured results showed that no significant difference was detected between the LDH activity of PDN and that of control, which implied the high viability of cell monolayer. Then, the effect of PDN on the F-actin filaments of the cell monolayer was measured under LCSM (Fig. 2b). The captured images showed that the F-actin filaments of negative control appeared as green continuous bands surrounding the cells. However, when the cell monolayers were incubated with different PDN, the green bands became discontinuous and seemed like necklace around the cells. These images showed that the integrity of cell monolayer could be broken by these PDNs and the fluidity of the cell membrane could be significantly increased, which could

Table II Pharmacokinetic Parameters of Probucol in Rats After Oral Administration of PDN and Free Drug Suspension (200 mg/kg, $n = 6$)

Parameters	Probucol	T_{20}-PDN	T_{80}-PDN	TP-PDN	HS-PDN
C_{max}(ng/mL)	47.2 ± 5.2	225.6 ± 69.6	459.5 ± 167.1	267.2 ± 52.3	559.3 ± 87.6
T_{max}(h)	7.3 ± 1.0	2.5 ± 0.6	2.0 ± 1.0	3.8 ± 1.5	3.0 ± 0
$AUC_{(0-t)}$(ng·h/mL)	1269 ± 115	3876 ± 629	5219 ± 485	6848 ± 1402	13135 ± 1693
$T_{1/2}$(h)	19.3 ± 7.8	15.0 ± 1.9	22.7 ± 8.4	18.6 ± 4.5	17.9 ± 0.8
Fr	–	3.0	4.1	5.4	10.4

be promising for enhancing its permeability across the intestinal membrane.

Absorption of PDN in the Intestine

The intestinal absorption of PDN was visualized under the *In Vivo* Imaging System (Carestream FX Pro, USA) after oral administration. HS-PDN was fluorescently labeled with a hydrophobic near infrared fluorescent DiR for visualization (Fig. 3a). The captured images of the intestine indicated that plenty of fluorescence (EX 730 nm, Em 790 nm) was detected in duodenum and jejunum at 1.0 h and 4.0 h after oral administration, and the fluorescent intensity was significantly decreased with time. It could be deduced that PDN was mainly absorbed in duodenum and jejunum after oral administration. Moreover, the absorption of PDN in the intestine was observed under LCSM. PDN was fluorescently labeled with Nile Red for the detection. By contrast, the actin filaments were stained with phalloidin-FITC (Green) and the nuclei was counterstained with DAPI (Blue) for the visualization (25). The captured images showed that much red fluorescence was visible in the intestine villi in PDN treated group, which located between the green and blue fluorescence in the intestine section (Fig. 3b). However, the red fluorescence signals were seldom detected in the images of free fluorescent dye group. Therefore, it could be deduced that the fluorescent PDN could be internalized into the enterocytes lining the intestine epithelium.

Table III Correlation Coefficient Between the *In Vitro* Properties and Increased Cellular Uptake or Improved Oral Bioavailability of Various PDN

PDN	MD (nm)	R_{LT}	R_{LT}/MD	$(R_{LT})^2$	$(R_{LT})^2$/MD
T_{20}-PDN	44.06	0.1629	3.697×10^{-3}	2.654×10^{-2}	0.602×10^{-3}
T_{80}-PDN	53.33	0.2153	4.037×10^{-3}	4.635×10^{-2}	0.869×10^{-3}
TP-PDN	66.34	0.2730	4.115×10^{-3}	7.453×10^{-2}	1.123×10^{-3}
HS-PDN	40.07	0.3125	7.799×10^{-3}	9.766×10^{-2}	2.437×10^{-3}
CCr	/	0.782	**0.997**	0.820	0.980
CFr	/	0.900	0.976	0.930	**0.999**

Bold and *underline* numbers mean the best correlation with *in vitro* parameter

MD Mean diameter of various PDN

R_{LT} Ratio of molecular weight of lipophilic unit compared to the total molecule weight of surfactant molecule involved in PDN

CCr Correlation coefficient of increased cellular uptake in Caco-2 cell monolayer of PDN and their *in vitro* properties

CFr Correlation coefficient of improved relative oral bioavailability of various PDN and their *in vitro* properties

In Vivo Pharmacokinetic Behavior

The *in vivo* pharmacokinetic behavior of various PDNs was performed in rats in comparison with that of free drug suspension to verify the effectiveness of PDN in enhancing the oral bioavailability of insoluble drugs. The measured results indicated that the significant difference occurred between the plasma concentration-time profiles of various PDNs and that of free drug suspension (Fig. 4). At each of the time points after oral administration, the plasma concentration of probucol from PDN was obviously higher than that from free probucol suspension. Moreover, the significant difference was detected among the plasma concentration of probucol from each PDN. The pharmacokinetic parameters of various PDNs and free probucol were calculated and illustrated in Table II. Typically, compared with the free drug suspension, the peak concentration (C_{max}) of probucol from T_{20}-PDN, T_{80}-PDN, TP-PDN, HS-PDN, was significantly increased by 4.8, 9.7, 5.7 and 11.8-fold, respectively, while the time to C_{max} (T_{max}) was significantly shortened. In particular, the relative oral bioavailability of probucol from these PDNs was improved 3.0, 4.1, 5.4 and 10.4 folds, respectively. Thereby, the oral bioavailability of probucol was obviously improved by the directed self-assembled nanoparticles, which effectively verified the validity of PDN in enhancing the oral delivery of water-insoluble drugs.

Inherent Correlation

The experimental results indicated the cellular uptake of probucol in Caco-2 cell monolayer and its oral bioavailability were greatly improved by PDN. The correlation analysis was performed between the relative cellular uptake (Cr) or relative oral bioavailability (Fr) of these PDN and their *in vitro* physicochemical properties. The selected *in vitro* parameters of PDN including R_{LT}, R_{LT}/MD, $(R_{LT})^2$ and $(R_{LT})^2$/MD were listed in Table III. The linear regression analysis was showed in Fig. 5 and the correlation coefficient was calculated in Table III. In the regression analysis of relative cellular uptake

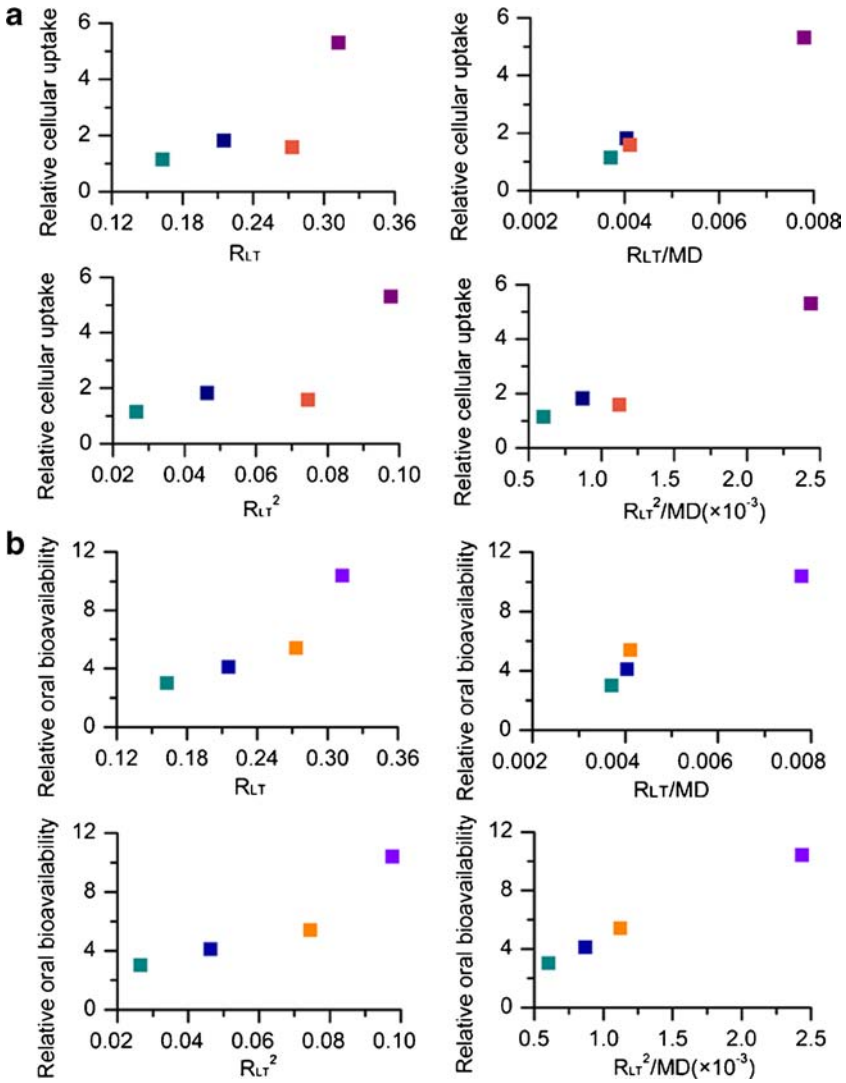

Fig. 5 Inherent correlation between the relative cellular uptake in Caco-2 cell monolayer (**a**) or relative oral bioavailability (**b**) of various PDN and their *in vitro* physicochemical properties.

and *in vitro* parameters, the correlation coefficient was the highest of 0.997 for the parameter R_{LT}/MD (Fig. 5a, Table III). On the other hand, between the relative oral bioavailability and *in vitro* parameters, the correlation coefficient reached the highest of 0.999 for $(R_{LT})^2/MD$ (Fig. 5b, Table III). Accordingly, the enhancement of cellular uptake in Caco-2 cell monolayer by PDN could be most linearly correlated with the parameter of R_{LT}/MD (Fig. 5a), while the improvement of oral bioavailability could be most correlated with $(R_{LT})^2/MD$ (Fig. 5b). Thereby, the enhancement of cellular uptake and oral delivery of insoluble probucol by PDN could be significantly affected by both the characters of the involved surfactants and the particle size of the directed self-assembled nanoparticles.

DISCUSSION

Oral delivery remains the most preferred route of drug administration for the treatment of many chronic diseases (3,5,13,26). It is well-known that the therapeutic efficacy of a drug molecule significantly depends on its adequate systemic exposure after oral administration. However, about 30–40% of commercial drugs and new chemical entities are poorly water-soluble drugs and show too low oral bioavailability to bring about satisfactory therapeutic efficacy (6). As a consequence of modern drug discovery techniques, the number of pharmacologically active compounds has increased significantly (1). Unfortunately, almost 70% of these potential drug candidates is very poorly soluble in water and has to be discarded due to their poor absorption before reached the pharmaceutics departments (5). Thereby, the improvement of aqueous solubility and oral absorption of water-insoluble drugs could be an essential prerequisite for the achievements of the pharmacological effects.

The poor oral absorption of water-insoluble drugs could mainly result from the poor solubility in the milieu of the GI tract and the limited permeability across the intestinal membrane (1,2,27,28). Nanoparticles have demonstrated great

potential for enhancing the aqueous solubility and oral bioavailability of lipophilic drugs. The lipophilic drugs are commonly encapsulated into the core of lipid or polymeric nanoparticles (1–3,7,13). Herein, we hypothesized that the highly lipophilic probucol and hydrophobic units of surfactants could be directed into nanoparticles due to the intermolecular hydrophobic interactions, which were verified by TEM images and DLS measurements. It has been reported that probucol nanoparticles formulated with polyvinylpyrrolidone (PVP) and sodium dodecyl sulphate (SDS) had been developed by grinding method with great improvement of oral bioavailability (29–31). In this study, probucol loaded nanoparticles was formulated only one surfactant in each PDN, and prepared by a self-assembled technique. The measured results indicated that PDN had good stability in the mimicked GI fluids of 0.1 M HCl (pH 1.2) or phosphate buffered solution (pH 6.8). Moreover, the solubility of probucol in water was remarkably increased over 2×10^6-fold after its assembly into PDN. Accordingly, the greatly increased aqueous solubility of probucol by PDN and its favorable stability in GI fluids could facilitate its transport across the intestinal barrier (1,2).

Then, the cellular uptake of PDN in Caco-2 cell monolayer was respectively enhanced 1.15, 1.82, 1.59 and 5.31-fold by serious PDN of T_{20}-PDN, T_{80}-PDN, TP-PDN and HS-PDN. Moreover, the oral bioavailability of insoluble probucol was significantly improved 3.0, 4.1, 5.4 and 10.4 fold. These improvements of cellular uptake and oral bioavailability were correlated with the physical properties of involved surfactants and mean diameters of PDN. Thereby, the possible reason for significant differences in the performance of different PDN nanoparticles could attribute to the hydrophobic ratio in these surfactant molecules and formation of nanoparticles. Previous results had indicated that the enhancement of oral delivery by a nanocarrier was greatly affected by the physiological barrier, such as the stability in the GI medium, diffusion across the unstirred water layer, transport across the intestinal epithelium (1,3,26). Accordingly, the obviously enhanced oral delivery by PDN could result from their unique physicochemical properties and advantages. Firstly, the *in vitro* characterizations verified the good stability of PDN in the mimicked GI fluids, which could be beneficial for the diffusion across the barrier of unstirred water layer to the mucus of GI tract. Secondly, the involved surfactant of Tween 20, Tween 80, TPGS and HS-15 in PDN could promote the adhesion and affinity of PDN to the intestinal tract (19,25,32,33). Thirdly, the nanometer-sized PDN could improve the accessibility to the intestinal mucus and adhesion to the enterocytes surface, enhance their uptake in the enterocytes, thereby facilitating its permeation across the intestinal barriers (1,2,33,34). Thereby, the directed self-assembled nanoparticles could provide an effective and promising platform for enhancing its oral delivery of hydrophobic drugs.

CONCLUSION

Probucol loaded nanoparticles were developed by directed self-assembly technique to improve the oral delivery. The experimental results indicated that the cellular uptake of probucol in Caco-2 cell monolayer and its oral bioavailability in rats were greatly improved by various PDN. The significant enhancements were correlated with the physicochemical properties of these nanoparticles. Thereby, the directed self-assembly could provide a new strategy for enhancing the oral delivery of hydrophobic drugs.

ACKNOWLEDGMENTS AND DISCLOSURES

Zhiwen Zhang and Shijun Jiang contributed equally to this work.

The National Basic Research Program of China (2013CB932503 and 2013CB932704), the National Natural Science Foundation of China (81270047, 81373359) and SA-SIBS Scholarship Program are gratefully acknowledged for financial support.

REFERENCES

1. Porter CJ, Trevaskis NL, Charman WN. Lipids and lipid-based formulations: optimizing the oral delivery of lipophilic drugs. Nat Rev Drug Discov. 2007;6(3):231–48.
2. Ensign LM, Cone R, Hanes J. Oral drug delivery with polymeric nanoparticles: the gastrointestinal mucus barriers. Adv Drug Deliv Rev. 2012;64(6):557–70.
3. Zhang Z, Gao F, Jiang S, Ma L, Li Y. Nano-based drug delivery system enhances the oral absorption of lipophilic drugs with extensive presystemic metabolism. Curr Drug Metab. 2012;13(8):1110–8.
4. Mu H, Holm R, Mullertz A. Lipid-based formulations for oral administration of poorly water-soluble drugs. Int J Pharm. 2013;453(1):215–24.
5. Cooper ER. Nanoparticles: a personal experience for formulating poorly water soluble drugs. J Control Release. 2010;141(3):300–2.
6. Zhang Z, Huang Y, Gao F, Gao Z, Bu H, Gu W, *et al.* A self-assembled nanodelivery system enhances the oral bioavailability of daidzein: in vitro characteristics and in vivo performance. Nanomedicine (London). 2011;6(8):1365–79.
7. Zhang ZW, Bu HH, Gao ZW, Huang Y, Gao F, Li YP. The characteristics and mechanism of simvastatin loaded lipid nanoparticles to increase oral bioavailability in rats. Int J Pharm. 2010;394(1–2):147–53.
8. Grzelczak M, Vermant J, Furst EM, Liz-Marzan LM. Directed self-assembly of nanoparticles. ACS Nano. 2010;4(7):3591–605.
9. Zhao Y, Thorkelsson K, Mastroianni AJ, Schilling T, Luther JM, Rancatore BJ, *et al.* Small-molecule-directed nanoparticle assembly towards stimuli-responsive nanocomposites. Nat Mater. 2009;8(12):979–85.
10. Zhang P, Cheetham AG, Lin YA, Cui H. Self-assembled tat nanofibers as effective drug carrier and transporter. ACS Nano. 2013;7(7):5965–77.
11. Sanchez-Iglesias A, Grzelczak M, Altantzis T, Goris B, Perez-Juste J, Bals S, *et al.* Hydrophobic interactions modulate self-assembly of nanoparticles. ACS Nano. 2012;6(12):11059–65.

12. Wang W, Chau Y. Efficient and facile formation of two-component nanoparticles via aromatic moiety directed self-assembly. Chem Commun. 2011;47(37):10224–6.
13. Date AA, Desai N, Dixit R, Nagarsenker M. Self-nanoemulsifying drug delivery systems: formulation insights, applications and advances. Nanomedicine (London). 2010;5(10):1595–616.
14. Xia DN, Cui FD, Piao HZ, Cun DM, Piao HY, Jiang YB, *et al.* Effect of crystal size on the in vitro dissolution and oral absorption of nitrendipine in rats. Pharm Res. 2010;27(9):1965–76.
15. Zhang ZW, Huang J, Jiang SJ, Liu ZY, Gu WW, Yu HJ, *et al.* Porous starch based self-assembled nano-delivery system improves the oral absorption of lipophilic drug. Int J Pharm. 2013;444(1–2):162–8.
16. Thakuria R, Delori A, Jones W, Lipert MP, Roy L, Rodriguez-Hornedo N. Pharmaceutical cocrystals and poorly soluble drugs. Int J Pharm. 2013;453(1):101–25.
17. Yamashita S, Matsuzawa Y. Where are we with probucol: a new life for an old drug? Atherosclerosis. 2009;207(1):16–23.
18. Heeg JF, Hiser MF, Satonin DK, Rose JQ. Pharmacokinetics of probucol in male-rats. J Pharm Sci. 1984;73(12):1758–63.
19. Gao F, Zhang Z, Bu H, Huang Y, Gao Z, Shen J, *et al.* Nanoemulsion improves the oral absorption of candesartan cilexetil in rats: performance and mechanism. J Control Release. 2011;149(2):168–74.
20. Rizza L, Frasca G, Nicholls M, Puglia C, Cardile V. Caco-2 cell line as a model to evaluate mucoprotective proprieties. Int J Pharm. 2012;422(1–2):318–22.
21. Zhang Z, Gao F, Jiang S, Chen L, Liu Z, Yu H, *et al.* Bile salts enhance the intestinal absorption of lipophilic drug loaded lipid nanocarriers: mechanism and effect in rats. Int J Pharm. 2013;452(1–2):374–81.
22. Xin H, Chen L, Gu J, Ren X, Wei Z, Luo J, *et al.* Enhanced anti-glioblastoma efficacy by PTX-loaded PEGylated poly(varepsilon-caprolactone) nanoparticles: in vitro and in vivo evaluation. Int J Pharm. 2010;402(1–2):238–47.
23. Zhang L, Yao J, Zhou JP, Wang T, Zhang Q. Glycyrrhetinic acid-graft-hyaluronic acid conjugate as a carrier for synergistic targeted delivery of antitumor drugs. Int J Pharm. 2013;441(1–2):654–64.
24. Nassar T, Rom A, Nyska A, Benita S. A novel nanocapsule delivery system to overcome intestinal degradation and drug transport limited absorption of P-glycoprotein substrate drugs. Pharm Res. 2008;25(9):2019–29.
25. Zhang Z, Ma L, Jiang S, Liu Z, Huang J, Chen L, *et al.* A self-assembled nanocarrier loading teniposide improves the oral delivery and drug concentration in tumor. J Control Release. 2013;166(1):30–7.
26. Roger E, Lagarce F, Garcion E, Benoit JP. Biopharmaceutical parameters to consider in order to alter the fate of nanocarriers after oral delivery. Nanomedicine (London). 2010;5(2):287–306.
27. Larsen AT, Akesson P, Jureus A, Saaby L, Abu-Rmaileh R, Abrahamsson B, *et al.* Bioavailability of cinnarizine in dogs: effect of SNEDDS loading level and correlation with cinnarizine solubilization during in vitro lipolysis. Pharm Res. 2013. doi:10.1007/s11095-013-1145-x.
28. Memvanga PB, Eloy P, Gaigneaux EM, Preat V. In vitro lipolysis and intestinal transport of beta-arteether-loaded lipid-based drug delivery systems. Pharm Res. 2013;30(10):2694–705.
29. Pongpeerapat A, Wanawongthai C, Tozuka Y, Moribe K, Yamamoto K. Formation mechanism of colloidal nanoparticles obtained from probucol/PVP/SDS ternary ground mixture. Int J Pharm. 2008;352(1–2):309–16.
30. Pongpeerapat A, Higashi K, Tozuka Y, Moribe K, Yamamoto K. Molecular interaction among probucol/PVP/SDS multicomponent system investigated by solid-state NMR. Pharm Res. 2006;23(11):2566–74.
31. Fukami T, Ishii T, Io T, Suzuki N, Suzuki T, Yamamoto K, *et al.* Nanoparticle processing in the solid state dramatically increases the cell membrane permeation of a cholesterol-lowering drug, probucol. Mol Pharm. 2009;6(3):1029–35.
32. Zhang Z, Gao F, Bu H, Xiao J, Li Y. Solid lipid nanoparticles loading candesartan cilexetil enhance oral bioavailability: in vitro characteristics and absorption mechanism in rats. Nanomedicine: NBM. 2012;8(5):740–7.
33. Kulkarni SA, Feng SS. Effects of particle size and surface modification on cellular uptake and biodistribution of polymeric nanoparticles for drug delivery. Pharm Res. 2013;30(10):2512–22.
34. Yanez JA, Wang SW, Knemeyer IW, Wirth MA, Alton KB. Intestinal lymphatic transport for drug delivery. Adv Drug Deliv Rev. 2011;63(10–11):923–42.